Published in final edited form as:

Cancer Res. 2017 May 01; 77(9): 2401–2412. doi:10.1158/0008-5472.CAN-16-2922.

Genetic manipulation of *Helicobacter pylori* Virulence Function by Host Carcinogenic Phenotypes

Giovanni Suarez[1], **Judith Romero-Gallo**[1], **Johanna C. Sierra**[1], **M. Blanca Piazuelo**[1], **Uma S. Krishna**[1], **Martin A. Gomez**[2,3], **Keith T. Wilson**[1], and **Richard M. Peek Jr.**[1,*]

[1]Departments of Cancer Biology, Pathology, Microbiology, and Immunology, and Medicine, Vanderbilt University Medical Center, Nashville, TN.

[2]National University of Colombia, Department of Medicine

[3]Hospital El Tunal Unit of Gastroenterology, Bogota, Colombia.

Abstract

Helicobacter pylori is the strongest risk factor for gastric adenocarcinoma, yet only a minority of infected persons ever develop this malignancy. One cancer-linked locus is the *cag* type 4 secretion system (*cag*T4SS), which translocates an oncoprotein into host cells. A structural component of the *cag*T4SS is CagY, which become rapidly altered during *in vivo* adaptation in mice and rhesus monkeys, rendering the *cag*T4SS nonfunctional; however, these models rarely develop gastric cancer. We previously demonstrated that the *H. pylori cag*$^+$ strain 7.13 rapidly induces gastric cancer in Mongolian gerbils. We now use this model, in conjunction with samples from patients with premalignant lesions, to define the effects of a carcinogenic host environment on the virulence phenotype of *H. pylori* to understand how only a subset of infected individuals develop cancer. *H. pylori cag Y* sequence differences and *cag*T4SS function were directly related to the severity of inflammation in human gastric mucosa in either a synchronous or metachronous manner. Serial infections of Mongolian gerbils with *H. pylori* strain 7.13 identified an oscillating pattern of *cag*T4SS function. The development of dysplasia or cancer selected for attenuated virulence phenotypes, but robust *cag*T4SS function could be restored upon infection of new hosts. Changes in the genetic composition of *cag Y* mirrored *cag*T4SS function, although the mechanisms of *cag Y* alterations differed in human isolates (mutations) versus gerbil isolates (addition/deletion of motifs). These results indicate that host carcinogenic phenotypes modify *cag*T4SS function via altering *cag Y*, allowing the bacteria to persist and induce carcinogenic consequences in the gastric niche.

Introduction

Infection with *Helicobacter pylori* is the strongest known risk factor for gastric cancer, a disease that claims >700,000 lives per year (1), yet the precise mechanisms that regulate cancer development in response to this pathogen are less well defined. In many regions of

*Corresponding Author: Richard Peek, 2215 Garland Avenue, Nashville, TN, 37232-2279. Phone: 615-322-5200; Fax: 615-343-6229; richard.peek@vanderbilt.edu. .

Conflicts of Interest: None

the world, the rates of *H. pylori* infection and gastric cancer are concordant; however, this association is not universal. In Colombia, the prevalence of *H. pylori* is very high throughout the country, but individuals residing in the mountains have high rates of gastric cancer, whereas those on the coast have very low rates (2). Kodaman *et al.* recently showed that specific interactions between microbial and human genetic ancestries clearly predicted the risk for gastric cancer in Colombia (3). These findings indicate that aberrant co-evolution between *H. pylori* and its host may affect pathogenesis.

One specific cancer-linked *H. pylori* locus is the *cag* pathogenicity island (*cag*PAI), which encodes a type IV secretion system (T4SS) that translocates the oncoprotein CagA, peptidoglycan, and DNA into host cells (4-6). A structural component of the *cag*T4SS is CagY, which is required for NF-κB-driven pro-inflammatory cytokine secretion. *cagY* encodes for an ~1900 amino acid protein, which is susceptible to rearrangements, compromising the length and function of the protein. Previous studies have shown that CagY can become rapidly altered during *in vivo* adaptation in mice and Rhesus monkeys, raising the hypothesis that CagY can mediate evasion of the host immune response (7,8). However, these models rarely develop gastric cancer. In contrast, infection of Mongolian gerbils with *H. pylori* leads to gastric adenocarcinoma in approximately 60% of infected animals (9-12).

To address the hypothesis that a carcinogenic environment within the stomach alters *H. pylori* virulence, we first utilized a unique set of paired *H. pylori* clinical isolates (13). Archival and recent *H. pylori* strain J99 are human clinical strains isolated from a single patient that underwent endoscopy six years apart. During this time period, a shift occurred in the pattern of *H. pylori*-induced inflammation in this patient, from antral-predominant to corpus-predominant gastritis, a crucial step in the cascade to gastric carcinogenesis (14). We now use these unique samples, in conjunction with the Mongolian gerbil model of cancer, to define the effects of a carcinogenic host environment on the virulence phenotype of *H. pylori* as a means to understand how only a subset of infected individuals develop gastric cancer in response to this pathogen.

Materials and Methods

Bacterial strains

H. pylori strains were maintained on TSA-blood agar plates. Liquid cultures were prepared in Brucella broth supplemented with 10% newborn calf serum. The nomenclature for all *in vivo*-adapted strains derived from parental *H. pylori* strain 7.13 is contained in Supplementary Figure S1.

Bacterial-epithelial cell co-cultures

AGS cells (CRL-1739) were obtained from ATCC and maintained in RPMI-1640 supplemented with 10% fetal bovine serum under standard growth conditions. ATCC fully authenticated these cells by Short Tandem Repeat (STR) DNA profiling. After purchase, low passage vials were frozen and maintained in liquid nitrogen for future use. AGS cells were co-cultured with *H. pylori* at a MOI of 30 for CagA translocation assays or a MOI of 10 for NF-κB assays for all strains included in this study.

Rodent infections and histopathology

Mongolian gerbils were challenged with *H. pylori* for up to 16 weeks as previously described (5,15). Gastric tissues were harvested and gastric injury and quantitative *H. pylori* cultures were assessed as described (5).

RFLP

PCR products of *cagY*, *cagA*, or components of the *cag*PAI from *H. pylori* strains were digested with *DdeI* or *HinfI* at 37°C and separated in a 6-9% polyacrylamide gradient gel. Images from stained gels were acquired using a Biorad ChemiDoc analyzer.

Human samples

Archival and recent *H. pylori* J99 strain were isolated from gastric biopsy specimens from a single patient six years apart (13). Gastric antrum and corpus biopsies from seven additional patients were obtained via endoscopy. Gastric inflammation and quantitative *H. pylori* cultures were assessed as described (16).

Statistical analysis

The Mann–Whitney test and one-way ANOVA with a Newman–Keuls post-test were used to compare data groups. Data were plotted and analyzed using Prism (GraphPad Inc).

Results

The *H. pylori* cancer-linked *cagY* locus harbors a high level of genetic variability

cagY contains 2 repeat domains which are susceptible to in-frame rearrangements compromising the length of the protein (Supplementary Fig S2). Sequence analysis of *cagY* from *H. pylori* strain 7.13 revealed the presence of two different motifs (Motif 2A and 2B, Consensus sequences shown in Supplementary Fig S3) within repeat region 2 (Supplementary Fig S2). This particular carcinogenic *H. pylori* strain has sixteen 2A motifs and six 2B motifs. We therefore used both RFLP and DNA sequence changes to identify *cagY* diversity among isolates used in this study.

Temporal changes in *cagY* rearrangements and *cag*T4SS function are directly related to severity of inflammation within an *H. pylori*-colonized human pre-malignant gastric environment

We first utilized paired *H. pylori* isolates (strain J99), separated in time by 6 years, that were obtained from the gastric antrum of a single patient. The patient did not receive any antibiotic eradication therapy targeting *H. pylori* during this time interval. In this patient, total inflammation scores in the gastric antrum were three-fold higher compared to scores in the corpus at the initial endoscopy ($p<0.05$); however, this pattern was reversed six years later as the severity of corpus inflammation was approximately three-fold higher compared to antral inflammation ($p<0.05$) (14). At the time of the repeat endoscopy, the gastric pH was 5.0, further indicating that acid secretion was impaired. The transition from antral-predominant to corpus-predominant gastritis suggested that this patient was progressing towards a hypochlorhydric phenotype and may be at a higher risk for intestinal-type gastric

adenocarcinoma, although he had not developed this malignancy at the time of the second endoscopy. *cagY* RFLP profiles differed when the archival J99 isolate was compared to the recent isolate (Fig 1A). Concordantly, *cagY* sequence analysis identified 24 single nucleotide polymorphisms (SNPs) when the archival and recent J99 strains were compared. Among the 24 SNPs, fourteen encoded synonymous changes and ten were non-synonymous (Supplementary Fig S4). Interestingly, 9 of the 10 non-synonymous SNPs were located in the *cagY* repeat domain 2 (Fig 1B). Comparison of the CagY secondary structures of the archival and recent J99 strains revealed that non-synonymous SNPs induced changes in the predicted secondary structures (Fig 1B).

To determine if differences in *cagY* were related to *cag*T4SS function, we quantified CagA translocation and NF-κB activation *in vitro*. Archival *H. pylori* J99, which was isolated from a highly inflamed micro-environment, translocated significantly higher levels of CagA compared to the recent *H. pylori* J99 isolate. These data mirrored differences in levels of NF-κB activation induced by these strains (Fig 1C). Thus, *cagY* sequence differences and *cag*T4SS function were directly related to the severity of inflammation in a patient who had progressed along a histological cascade towards gastric carcinogenesis.

Output strains from Mongolian gerbils infected with a *H. pylori cag*$^+$ carcinogenic strain contain different *cagY* rearrangements, which are linked to changes in *cag*T4SS function

Based on our results in the human stomach, we next determined the mode and stability of *cagY* and *cag*T4SS function in an *H. pylori* cancer model. Gerbils were infected with the prototype clonal *H. pylori cag*$^+$ carcinogenic strain 7.13 for 12 weeks (Supplementary Fig S1). Two *H. pylori* strains recovered from independent gerbils with disparate levels of inflammation and injury were then subjected to *cagY* RFLP analysis. RFLP profiles revealed variation between one output strain (7.13-2) when compared to the parental strain 7.13 or its sibling output strain 7.13-1 (Fig 2A). The ability of *H. pylori* output strain 7.13-2, which induced low inflammation *in vivo*, to translocate CagA or activate NF-κB was significantly attenuated compared to the parental input strain 7.13 or the adapted strain 7.13-1 (Fig 2B, 2C). These data indicate that rearrangements in *cagY* induced by prolonged *in vivo* adaptation in gerbils could modulate function of the *cag*T4SS.

Mongolian gerbils infected with *H. pylori* derivative strains harboring distinct *cagY* rearrangements develop different patterns of disease

To determine if adapted strains with polar *in vitro* phenotypes could differentially affect pathogenesis *in vivo*, new populations of gerbils were infected with the *H. pylori* derivative strains 7.13-1 or 7.13-2 (Supplementary Fig S1). All challenged animals were successfully colonized and there were no differences in colonization density between the groups. However, strain 7.13-1, which exhibited considerable potency for CagA translocation and NF-κB activation (Fig 2B, 2C), induced high levels of inflammation early (e.g., 8 weeks) post-infection. In contrast, strain 7.13-2 induced a delayed inflammatory response, which began to increase 12-16 weeks post-infection (Fig 3A). Pre-neoplastic lesions were also rapidly induced by strain 7.13-1, and 20% of animals had developed dysplasia 4 weeks post infection, and by 16 weeks post-infection, 80% of the 7.13-1-infected animals developed

dysplasia and/or adenocarcinoma. In contrast, only 12% of animals infected with strain 7.13-2 developed dysplasia by 16 weeks post-infection (Fig 3B).

The ability of *H. pylori* to translocate CagA and activate NF-κB *in vitro* is directly related to the *in vivo* inflammatory phenotype, but inversely related to cancer

Having demonstrated different patterns of injury, re-adapted output strains from gerbils infected with the *H. pylori* derivative strains 7.13-1 and 7.13-2 were then tested *in vitro* for *cag*T4SS function. Output isolates from animals infected with the more potent strain 7.13-1, displayed a statistically significant attenuation in the ability to translocate CagA (p=0.008) and activate NF-κB (p=0.004) over time (Fig 3C, 3D). In contrast, output strains isolated from animals infected with strain 7.13-2, maintained a relatively stable ability to translocate CagA and activate NF-κB for the duration of infection (Fig 3C, 3D). Importantly, there was an inverse relationship between the presence of cancer and *cag*T4SS function, suggesting that host carcinogenic phenotypes may modify the function of specific *H. pylori* constituents that have been associated with disease (Fig 3E).

Since *H. pylori* strains 7.13-1 and 7.13-2 exhibited different *cagY* RFLP patterns, we next determined if the differences observed in CagA translocation and NF-κB activation by the re-adapted derivatives of *H. pylori* strains 7.13-1 or 7.13-2 were similarly related to new polymorphisms within *cagY*. Re-adapted strains isolated from animals infected with *H. pylori* strain 7.13-2 for 16 weeks showed variations in *cagY* RFLP patterns. Two of the 7.13-2 derived strains (strains 2 and 6) harbored a hybrid RFLP profile containing features present in the profiles of both strains 7.13-1 and 7.13-2; two strains (strains 1 and 3) reverted their RFLP profile to a profile similar to the original parental strain 7.13; and three strains maintained the same profile as input strain 7.13-2 (Fig 3F). This level of variability mirrored the large variability in inflammatory scores in gerbils infected for 16 weeks by *H. pylori* strain 7.13-2 (Fig 3A). In contrast to this degree of variability, isolates from animals infected with *H. pylori* strain 7.13-1 showed fewer differences in *cagY* rearrangements. One 7.13-1 derived strain (strain 4) harbored an intermediate RFLP profile containing elements from strains 7.13-1 and 7.13-2, one (strain 8) had a unique RFLP profile, but six maintained the same profile as the input strain 7.13-1 (Fig 3F). Interestingly, the re-adapted strains that reverted their *cagY* profiles, also reverted their ability to translocate CagA and activate NF-κB *in vitro*. In terms of mucosal injury, all *H. pylori* strains that had *cagY* RFLP profiles similar to strain 7.13-1 induced high levels of inflammation, while strains that harbored *cagY* RFLP patterns similar to strain 7.13-2 induced low levels of inflammation. Of interest, strains that possessed unique RFLP patterns (e.g., distinct from either strain 7.13-1 or 7.13-2), induced intermediate levels of inflammation (Fig 3A, 3F).

Rearrangements in *cagY* play an essential role in modulating function of the *H. pylori cag*T4SS

Our previous results indicate that the ability of *H. pylori* to induce severe inflammation and gastric injury oscillates in this model of cancer, and this parallels changes in *cag*T4SS function. To determine the stability of *in vivo*-induced *cagY* alterations and *cag*T4SS function, we next selected two output strains from gerbils with the same inflammatory phenotype but which harbored polar *cag*T4SS function, and infected new populations of

gerbils for 16 weeks (Supplementary Fig S1). *H. pylori* strain 7.13-1-1 is an *in vivo*-adapted strain obtained from an animal infected for 16 weeks with input strain 7.13-1 and showed an attenuated ability to translocate CagA compared with its parental strain 7.13-1 (Fig 4A). Strain 7.13-2-7 is a derivative strain from an animal infected for 16 weeks with strain 7.13-2 and exhibited substantial potency in CagA translocation compared with its parental strain 7.13-2 (Fig 4A). The data shown in Fig 4B are inflammation scores from new populations of gerbils that were infected with either *H. pylori* strain 7.13-1 (parent of 7.13-1-1), strain 7.13-2 (parent of 7.13-2-7), strain 7.13-1-1, or strain 7.13-2-7 for 16 weeks. *In vivo*, the severity of inflammation was directly related to pre-inoculation *cag*T4SS function, as determined by CagA translocation, in contrast to strain ancestry. Animals infected with strains 7.13-1 or 7.13-2-7 developed higher injury scores compared to animals infected with strains 7.13-2 or 7.13-1-1 (Fig 4B, 4C).

To determine if changes in bacterial phenotypes occurred during these infections, we performed CagA translocation and NF-κB activation assays *in vitro*. Most of the derivative strains from gerbils infected with *H. pylori* strains 7.13-2 or 7.13-1-1 recovered the capacity to translocate CagA. Conversely, only a few strains isolated from animals infected with strains 7.13-1 or 7.13-2-7 lost the ability to translocate CagA (Fig 4D, 4E) and these changes in CagA translocation reflected the ability to induce NF-κB (Fig 4F).

There was a direct correlation between levels of CagA translocation and *cagY* profiles among strains isolated from gerbils infected with strain 7.13-1-1 (Fig 4D, 4G); however, this relationship was not present in strains isolated from gerbils infected with strain 7.13-2-7, as only one isolate (7.13-2-7-6) had a different *cagY* RFLP profile yet maintained the ability to translocate CagA (Fig 4D, 4G). Conversely, one strain (7.13-2-7-1) did not express CagA (Fig 4D), but harbored the same *cagY* RFLP profile of other strains than maintained the ability to express CagA, suggesting a different mechanism of regulation.

In vivo-adapted *H. pylori* strains are panmictic populations that harbor different *cagY* rearrangements

We next determined whether reversions of *cagY* genotypes are due to: 1) the presence of panmictic populations pre-populated with isolates harboring different rearrangements of *cagY* or 2) to *de novo* rearrangements acquired *in vivo*. To test this hypothesis, we isolated twelve single colonies from *H. pylori* adapted strains 7.13-1, 7.13-2, 7.13-1-10 and 7.13-2-16 (Supplementary Fig S1) and assessed *cagY* RFLP profiles. All single colonies from strain 7.13-1 had identical *cagY* RFLP patterns. Among single colonies from strains 7.13-2, 7.13-1-10 and 7.13-2-16, we identified the presence of clones with different *cagY* rearrangements (Fig 5A). In total, we found four different RFLP patterns among the collective single colonies. RFLP profiles of strain 7.13-1 single colonies are similar to the original archival strain 7.13; for strain 7.13-2 single colonies, one RFLP profile is similar to 7.13-1 (7.13-2^{sc3}) and two are different (7.13-2^{sc1} and 7.13-2^{sc2}). For strain 7.13-1-10 single colonies, one RFLP pattern is similar to strain 7.13-1 (7.13-1-10^{sc2}), and one is different (7.13-1-10^{sc1}). For strain 7.13-2-16, one RFLP pattern is similar to that of strain 7.13-1 (7.13-2-16^{sc1}) and one pattern is similar to that of strain 7.13-2^{sc1} (7.13-2-16^{sc2}) (Fig 5A).

We next sequenced *cagY* from each of these single colony strains. Compared with the parental *H. pylori* strain 7.13, sequence analysis identified differences in the number and order of 2A and 2B motifs within the *cagY* repeat region 2 (Fig 5B). Strain 7.13-1-10^{sc1} has a cluster deletion around amino acid 510, which involves the loss of two 2A motifs and two 2B motifs. Strains 7.13-2^{sc1}, 7.13-2^{sc2}, and 7.13-2-16^{sc2} have an addition of one 2A motif and one 2B motif around amino acid 800. In addition, strain 7.13-2^{sc2} also has a deletion that compromises one 2A motif around amino acid 1355. Strain 7.13-1-10^{sc2} has an addition of one 2A motif and one 2B motif around amino acid 1220, but this insertion was not detectable by RFLP. Sequences from strains 7.13-1^{sc1}, 7.13-2^{sc3}, and 7.13-2-16^{sc1} did not show any differences when compared with parental strain 7.13 (Fig 5B). When we compared the predicted secondary structure between single colony strains, the addition or deletion of motifs 2A and/or 2B predicted changes in the length of alpha-helices, as well as additions or deletions of beta sheets (Fig 5B). Of interest, the mechanism underpinning changes in *cagY* sequences was different in isolates adapted to gerbils (deletion and/or addition of entire motifs) when compared to changes seen in the human *H. pylori* J99 paired strains (SNPs) (Fig 1B).

We also examined *cag*T4SS function among single colony isolates with varying *cagY* profiles. *H. pylori* clones with identical *cagY* RFLP profiles induced similar levels of NF-κB activation; thus, clones 7.13-1^{sc1}, 7.13-1^{sc2}, 7.13-2^{sc3}, 7.13-1-10^{sc2}, and 7.13-2-16^{sc1}, which have RFLP patterns similar to the parental strain 7.13, induced the highest levels of NF-κB activation. In contrast, clones 7.13-2^{sc1} and 7.13-2-16^{sc2}, which harbor *cagY* profiles similar to strain 7.13-2, induced the lowest levels of NF-κB activation. Clones 7.13-2^{sc2} and 7.13-1-10^{sc1} had unique *cagY* rearrangements, with corresponding intermediate and low capacities to activate NF-κB, respectively (Fig 5A, 5C). The ability of each of these clones to translocate CagA into AGS cells mirrored their ability to activate NF-κB (Fig 5C, Supplementary Fig S5).

To exclude the possibility that changes in the *cag*PAI exogenous to *cagY* may affect the phenotypes of interest, we performed RFLP analysis of PCR amplicons that spanned the entire *cag*PAI, excluding *cagY*. Global *cag*PAI RFLP profiles from eight different single colony strains were identical (Supplementary Fig S6). To further interrogate the entire *cag*PAI, sequence analysis of the entire *cag*PAI from two single colony isolates with different CagA translocation phenotypes (7.13-1^{sc2} and 7.13-2^{sc1}) was performed (Supplementary Table S1). The only differences identified were within *cagY* (Supplementary Fig S7).

To further corroborate the role of *cagY* in modulation of *cag*PAI function, we genetically exchanged *cagY* among four different strains of *H. pylori* (two with high *cag*PAI phenotypes, 7.13-1^{sc2} and 7.13-2^{sc3}, and two with low *cag*PAI phenotypes, 7.13-2^{sc1} and 7.13-2^{sc2}) using the five different *cagY* rearrangements found in *H. pylori* single colonies (Fig 5B, Supplementary Fig S8). We found that independent of the *H. pylori* recipient background, CagA translocation and NF-κB activation phenotypes were restored or lost based upon the *cagY* phenotype of the donor (Fig 5D, 5E, Supplementary Fig S9). In addition, to define how more refined rearrangements in *cagY* motifs may affect *cag*PAI function, we exchanged *cagY* between two strains with polar *cag*PAI phenotypes,

7.13-2-16^{sc1} and 7.13-2-16^{sc2}, but which only differed in a single *cagY* domain 2A (Fig 5B, Supplementary Fig S10). We found that *cag*PAI function could be restored or lost based upon the donor *cagY* motif, implicating this motif in *cag*PAI function (Fig 5F).

Mongolian gerbils infected with *H. pylori* single colonies carrying unique *cagY* rearrangements develop differences in the severity of inflammation and disease

To determine whether *H. pylori* single colonies induced differences in disease based on *cagY* RFLP patterns, colonization and inflammation was assessed in gerbils infected with the *H. pylori* single colony isolates. All animals were successfully colonized with the exception of gerbils challenged with the single colony strain 7.13-2^{sc1}, for which no animals were colonized. Within colonized animals, bacterial density levels were similar (Fig 6A); however, histopathologic analysis revealed significant differences in inflammation. Gerbils infected with *H. pylori* single colony isolates carrying similar *cagY* rearrangements developed similar levels of inflammation (Fig 6B). Specifically, gerbils infected with *H. pylori* isolates 7.13-1^{sc1}, 7.13-2^{sc3}, 7.13-1-10^{sc2}, and 7.13-2-16^{sc1}, which have identical *cagY* RFLP profiles and induce robust CagA translocation (Fig 5A, 5C), induced high levels of inflammation (Fig 6B). In contrast, animals infected with isolates 7.13-2^{sc2}, 7.13-1-10^{sc1}, and 7.13-2-16^{sc2}, which harbor different *cagY* profiles and an attenuated ability to translocate CagA (Fig 5A, 5C), induced low levels of inflammation (Fig 6B).

Similar to levels of inflammation, only animals infected with strains carrying *cagY* rearrangements linked to robust CagA translocation developed neoplastic lesions (Fig 6C). In contrast, animals infected with strains carrying *cagY* rearrangements associated with attenuated levels of CagA translocation only developed gastritis (Fig 6C). These results reinforce the role that *cagY* exerts as a modulator of *cag*T4SS function.

We next analyzed the RFLP profiles of isolated strains. As expected, after 16 weeks isolated strains harbored differences in *cagY* compared to the input clonal *H. pylori* single colony isolates (Fig 6D); however, all of these rearrangements represented new RFLP patterns with varying capacities to activate NF-κB and translocate CagA (Fig 6E, 6F). Thus, infection with *H. pylori* single colonies harboring a variety of *cagY* RFLP profiles can lead to the generation of new *cagY* rearrangements.

H. pylori clinical isolates can harbor synchronous *cagY* rearrangements

We then validated *cagY* diversity observed in our gerbil model by using paired *H. pylori* clinical strains, harvested from 2 different sites (antrum and corpus) within the stomachs of 7 individual patients during a single endoscopy. For these paired sets of samples, two patients (4 and 12) harbored inflammation scores that were higher in the antrum than the corpus, and five patients (5, 9, 28, 42 and 44) harbored the reverse (Fig 7A). In terms of *cagY* RFLP profiles, strains isolated from patients 4, 5, 28, and 42 harbored different RFLP patterns, while paired isolates from the remaining patients harbored identical profiles (Fig 7B). Five of the seven patients harbored either atrophic gastritis or intestinal metaplasia, but there was no significant relationship between site-specific *cagY* RFLP patterns and premalignant lesions.

We next defined the distribution of *cagY* rearrangements among single colony isolates (n=12) harvested from patients 9, 12, 28, 42 and 44. Single colony isolates from the antrum and corpus from patients 9, 12, and 44 displayed no differences in *cagY* RFLP profiles. In contrast, there were 2 different *cagY* profiles within antral and corpus single colony isolates from patient 28 and 42. Single colony profiles from patient 28 and 42 were unequally distributed between the antrum and corpus, as the predominant clone in the antrum (patient 28: 8/11 colonies (83%); patient 42: 12/12 colonies (100%)) was the minority clone in the corpus (patient 28: 2/12 colonies (17%); patient 42: 6/12 colonies (50%)) (Fig 7C). Finally, we tested the ability of these isolates to translocate CagA and activate NF-κB *in vitro*. We found no differences between antrum and corpus isolates from patients 4, 9, 12, and 42. In contrast, there were significant differences in *cag*T4SS function between antrum and corpus *H. pylori* isolates from patients 5, 28, and 44 (Fig 7D). These results in *cag*T4SS function mirrored NF-κB activation *in vitro* (Fig 7E).

Discussion

Our current results indicate that *H. pylori* harbors the capacity to nimbly modify function of its primary virulence constituent during prolonged colonization in a rodent model of gastric carcinogenesis. Chronic infection in gerbils engenders a portfolio of *cagY* isoforms, which are selected in conjunction with the intensity of host inflammatory and carcinogenic phenotypes. Importantly, the development of dysplasia and cancer led to the emergence of attenuated *cag*T4SS phenotypes, but robust function could be restored following adaptation to new hosts. The versatility of *cagY* isoforms and *cag*T4SS function was also validated in both synchronous and metachronous paired human samples and different mechanisms of *cagY* alterations were identified via sequencing. Deletions and additions of entire motifs appeared to predominate in gerbils while the development of single base pair mutations predominated in human samples.

Infection of wild-type mice with *H. pylori cag*T4SS positive strains frequently leads to deletions within the *cag* island (17,18), and the mechanism underpinning *cag* dysfunction appears to be in-frame rearrangements in *cagY* (7). In contrast to mice, previous studies have shown that *H. pylori* wild-type *cag*$^+$ strains colonize gerbils well without loss of *cag* function (19,20). However, these studies did not examine extensive populations of adapted isolates harvested from a large number of infected gerbils. Our current study has examined changes in *cagY* and the *cag*T4SS in this model in much greater depth through the use of serially-passaged strains, investigations of both pools and single colony isolates, and validation in human samples. We now demonstrate that *H. pylori* strains within gerbil stomachs exist as panmictic populations and that *cag*T4SS function can be altered based on the severity of disease, which is in contrast to the near complete ablation of *cag*T4SS function in mice.

Can long-term serial infections modify gain or loss of *cag*T4SS function and what is the benefit for *H. pylori* to harbor mechanisms that can up- or down-regulate function of this locus? Our current data indicate that the presence of dysplasia or cancer is associated with reduced *cag*T4SS function. Therefore, we would predict that serial infections would not enhance CagA translocation and/or the ability to activate NF-κB if there is development of

these lesions. However, this needs to be tested formally in the future. In terms of serially infecting derivative strains with minimal *cag*T4SS function, our data in Figure 4 have shown that strain 7.13-1-1, a derivative strain with low *cag*T4SS function, when re-infected into gerbils, induces variability in inflammation scores, CagA translocation indices, and NF-κB activation levels (Fig 4B, 4D, 4E, and 4F). Based on our results investigating single colony isolates (Fig 6), we posit that this reflects a panmictic pool of clones with variable *cagY* function within pre-inoculation strain 7.13-1-1. In terms of strains that never acquire the ability to translocate CagA or activate NF-κB, our data in Figure 5 demonstrate that two derivative strains, 7.13-2^{sc1} and 7.13-2-16^{sc2}, have little if any ability to translocate CagA or activate NF-κB, and their *cagY* RFLP profiles are identical (Fig 5A). Therefore, we plan in future experiments to utilize these strains in long-term adaptation studies to more carefully discern whether chronic and repeated serial infections may lead to a gain of *cag*T4SS function. One downstream ramification of CagA translocation is acquisition of iron sources that fuel *H. pylori* replication (21). Under conditions of iron deprivation, therefore, it may be beneficial for *H. pylori* to augment function of the *cag*T4SS and deliver higher payloads of CagA into host epithelial cells. *H. pylori* also harbors multiple pathogen-associated molecular patterns (PAMPs) that interact differently with innate immune receptors than the respective counterparts in other mucosal pathogens. *H. pylori* FlaA is a non-inflammatory molecule in terms of its ability to activate TLR5 (22). *H. pylori* LPS contains an anergic lipid A core that induces an attenuated TLR4-mediated response (23,24). We and others have shown that deacetylation of peptidoglycan allows *H. pylori* to evade host clearance (5,25-27). Thus, *H. pylori* has evolved to express an array of diverse phenotypes to subvert obstacles presented by the host (28), and the ability of *H. pylori* to alter *cagY* genotypes is yet another mechanism within the repertoire of this organism to evade host defenses.

In conclusion, we have utilized a robust rodent model of gastric cancer that closely recapitulates human disease to define alterations in *H. pylori* pathogenesis *in vivo*. Our findings demonstrate that *cag*T4SS function is typically maintained during prolonged colonization in this model but that the intensity of *cag*T4SS function can vary and is related to host disease phenotypes. *cagY* genotypes are altered concordant with *cag*T4SS function and can similarly vary in paired human samples obtained from different regions of the stomach or separated in time. The use of this model will facilitate more detailed investigations in the future that can identify new targets and therapeutic strategies to reduce the risk of cancer associated with this pathogen.

Supplementary Material

Refer to Web version on PubMed Central for supplementary material.

Acknowledgments

Financial Support: NIH R01-DK58587, R01-CA77955, P01-CA116087, P30-DK058404, P01-CA028842.

References

1. Hardbower DM, Peek RM Jr. Wilson KT. At the Bench: Helicobacter pylori, dysregulated host responses, DNA damage, and gastric cancer. J Leukoc Biol. 2014; 96(2):201–12. [PubMed: 24868089]
2. Correa P, Cuello C, Duque E, Burbano LC, Garcia FT, Bolanos O, et al. Gastric cancer in Colombia. III. Natural history of precursor lesions. J Natl Cancer Inst. 1976; 57(5):1027–35. [PubMed: 1003539]
3. Kodaman N, Pazos A, Schneider BG, Piazuelo MB, Mera R, Sobota RS, et al. Human and Helicobacter pylori coevolution shapes the risk of gastric disease. Proc Natl Acad Sci U S A. 2014; 111(4):1455–60. [PubMed: 24474772]
4. Varga MG, Shaffer CL, Sierra JC, Suarez G, Piazuelo MB, Whitaker ME, et al. Pathogenic Helicobacter pylori strains translocate DNA and activate TLR9 via the cancer-associated cag type IV secretion system. Oncogene. 2016
5. Suarez G, Romero-Gallo J, Piazuelo MB, Wang G, Maier RJ, Forsberg LS, et al. Modification of Helicobacter pylori peptidoglycan enhances NOD1 activation and promotes cancer of the stomach. Cancer Res. 2015; 75(8):1749–59. [PubMed: 25732381]
6. Viala J, Chaput C, Boneca IG, Cardona A, Girardin SE, Moran AP, et al. Nod1 responds to peptidoglycan delivered by the Helicobacter pylori cag pathogenicity island. Nat Immunol. 2004; 5(11):1166–74. [PubMed: 15489856]
7. Barrozo RM, Cooke CL, Hansen LM, Lam AM, Gaddy JA, Johnson EM, et al. Functional plasticity in the type IV secretion system of Helicobacter pylori. PLoS Pathog. 2013; 9(2):e1003189. [PubMed: 23468628]
8. Barrozo RM, Hansen LM, Lam AM, Skoog EC, Martin ME, Cai LP, et al. CagY is an immune-sensitive regulator of the Helicobacter pylori type IV secretion system. Gastroenterology. 2016
9. Watanabe T, Tada M, Nagai H, Sasaki S, Nakao M. Helicobacter pylori infection induces gastric cancer in Mongolian gerbils. Gastroenterology. 1998; 115(3):642–8. [PubMed: 9721161]
10. Honda S, Fujioka T, Tokieda M, Satoh R, Nishizono A, Nasu M. Development of Helicobacter pylori-induced gastric carcinoma in Mongolian gerbils. Cancer Res. 1998; 58(19):4255–9. [PubMed: 9766647]
11. Ogura K, Maeda S, Nakao M, Watanabe T, Tada M, Kyutoku T, et al. Virulence factors of Helicobacter pylori responsible for gastric diseases in Mongolian gerbil. J Exp Med. 2000; 192(11):1601–10. [PubMed: 11104802]
12. Zheng Q, Chen XY, Shi Y, Xiao SD. Development of gastric adenocarcinoma in Mongolian gerbils after long-term infection with Helicobacter pylori. J Gastroenterol Hepatol. 2004; 19(10):1192–8. [PubMed: 15377299]
13. Israel DA, Salama N, Krishna U, Rieger UM, Atherton JC, Falkow S, et al. Helicobacter pylori genetic diversity within the gastric niche of a single human host. Proc Natl Acad Sci U S A. 2001; 98(25):14625–30. [PubMed: 11724955]
14. Krishna U, Romero-Gallo J, Suarez G, Azah A, Krezel AM, Varga MG, et al. Genetic evolution of a Helicobacter pylori acid-sensing histidine kinase and gastric disease. J Infect Dis. 2016; 214(4): 644–8. [PubMed: 27190191]
15. Franco AT, Israel DA, Washington MK, Krishna U, Fox JG, Rogers AB, et al. Activation of beta-catenin by carcinogenic Helicobacter pylori. Proc Natl Acad Sci U S A. 2005; 102(30):10646–51. [PubMed: 16027366]
16. Sicinschi LA, Correa P, Peek RM, Camargo MC, Piazuelo MB, Romero-Gallo J, et al. CagA C-terminal variations in Helicobacter pylori strains from Colombian patients with gastric precancerous lesions. Clin Microbiol Infect. 2010; 16(4):369–78. [PubMed: 19456839]
17. Philpott DJ, Belaid D, Troubadour P, Thiberge JM, Tankovic J, Labigne A, et al. Reduced activation of inflammatory responses in host cells by mouse-adapted Helicobacter pylori isolates. Cell Microbiol. 2002; 4(5):285–96. [PubMed: 12064285]
18. Sozzi M, Crosatti M, Kim SK, Romero J, Blaser MJ. Heterogeneity of Helicobacter pylori cag genotypes in experimentally infected mice. FEMS Microbiol Lett. 2001; 203(1):109–14. [PubMed: 11557148]

19. Israel DA, Salama N, Arnold CN, Moss SF, Ando T, Wirth HP, et al. Helicobacter pylori strain-specific differences in genetic content, identified by microarray, influence host inflammatory responses. J Clin Invest. 2001; 107(5):611–20. [PubMed: 11238562]
20. Peek RM Jr. Wirth HP, Moss SF, Yang M, Abdalla AM, Tham KT, et al. Helicobacter pylori alters gastric epithelial cell cycle events and gastrin secretion in Mongolian gerbils. Gastroenterology. 2000; 118(1):48–59. [PubMed: 10611153]
21. Tan S, Noto JM, Romero-Gallo J, Peek RM Jr. Amieva MR. Helicobacter pylori perturbs iron trafficking in the epithelium to grow on the cell surface. PLoS Pathog. 2011; 7(5):e1002050. [PubMed: 21589900]
22. Gewirtz AT, Yu Y, Krishna US, Israel DA, Lyons SL, Peek RM Jr. Helicobacter pylori flagellin evades toll-like receptor 5-mediated innate immunity. J Infect Dis. 2004; 189(10):1914–20. [PubMed: 15122529]
23. Perez-Perez GI, Shepherd VL, Morrow JD, Blaser MJ. Activation of human THP-1 cells and rat bone marrow-derived macrophages by Helicobacter pylori lipopolysaccharide. Infect Immun. 1995; 63(4):1183–7. [PubMed: 7890370]
24. Ogawa T, Suda Y, Kashihara W, Hayashi T, Shimoyama T, Kusumoto S, et al. Immunobiological activities of chemically defined lipid A from Helicobacter pylori LPS in comparison with Porphyromonas gingivalis lipid A and Escherichia coli-type synthetic lipid A (compound 506). Vaccine. 1997; 15(15):1598–605. [PubMed: 9364689]
25. Wang G, Olczak A, Forsberg LS, Maier RJ. Oxidative stress-induced peptidoglycan deacetylase in Helicobacter pylori. J Biol Chem. 2009; 284(11):6790–800. [PubMed: 19147492]
26. Wang G, Maier SE, Lo LF, Maier G, Dosi S, Maier RJ. Peptidoglycan deacetylation in Helicobacter pylori contributes to bacterial survival by mitigating host immune responses. Infect Immun. 2010; 78(11):4660–6. [PubMed: 20805339]
27. Boneca IG, Dussurget O, Cabanes D, Nahori MA, Sousa S, Lecuit M, et al. A critical role for peptidoglycan N-deacetylation in Listeria evasion from the host innate immune system. Proc Natl Acad Sci U S A. 2007; 104(3):997–1002. [PubMed: 17215377]
28. Lina TT, Alzahrani S, Gonzalez J, Pinchuk IV, Beswick EJ, Reyes VE. Immune evasion strategies used by Helicobacter pylori. World J Gastroenterol. 2014; 20(36):12753–66. [PubMed: 25278676]

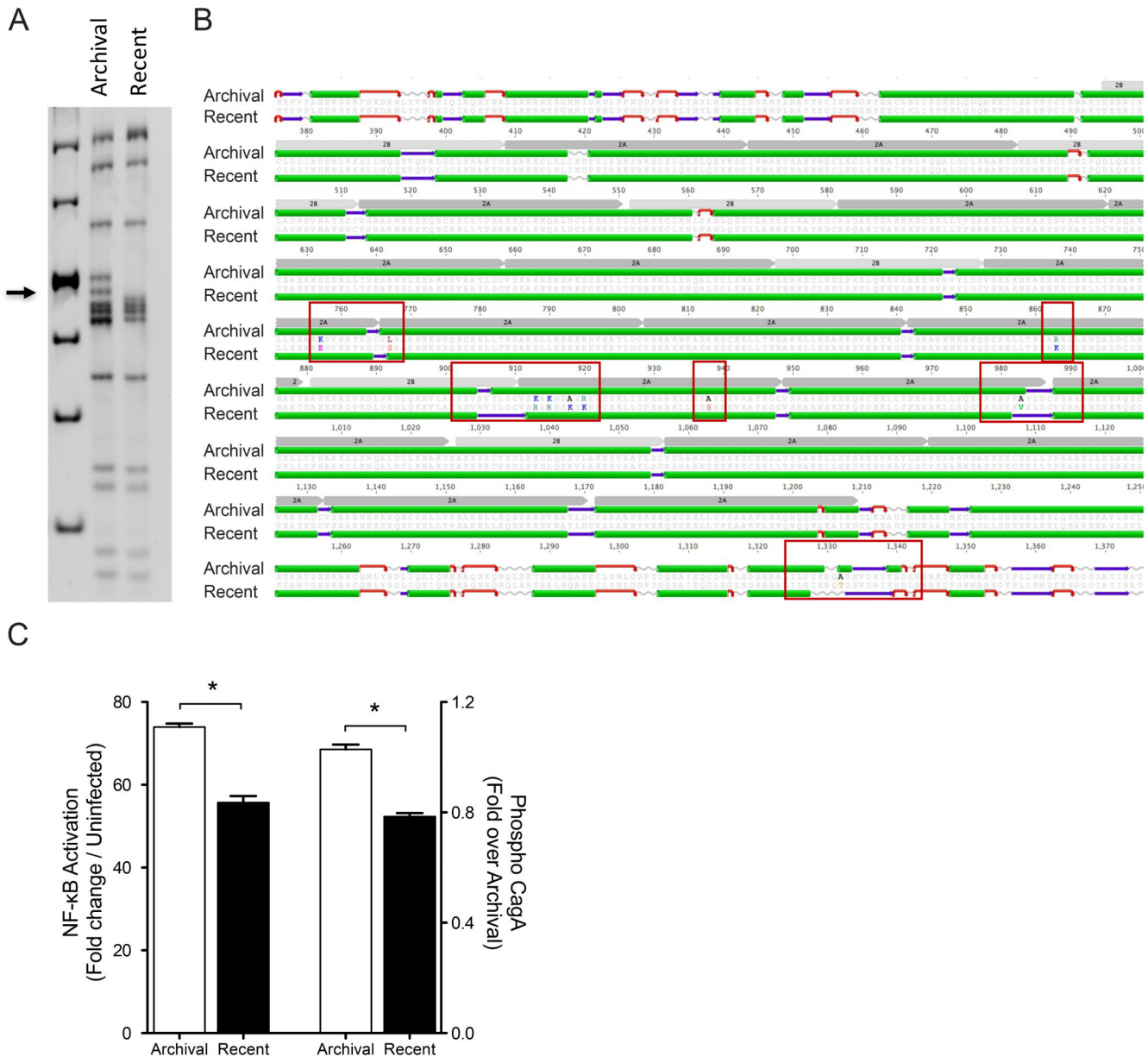

Fig 1. Relationship between *cagY* SNPs and *cag*T4SS function in paired human *H. pylori* isolates

(A) *cagY* RFLP profile of archival and recent *H. pylori* J99 strains. Arrow indicates area with different bands. (**B)** Alignment and predicted secondary structure of CagY of archival and recent J99 strains highlighting amino acid substitutions between strains and predicted changes in secondary structure (red boxes). Green: alpha helix; purple: beta-sheets; and red: beta turns. Repeat motifs 2A and 2B are shown in gray. (**C)** NF-κB activation (Left axis) and CagA translocation (Right axis) in AGS cells following co-culture with archival and recent J99 strains. Values are reported as a fold change over uninfected controls (NF-κB) or archival J99 (CagA translocation). Translocation is shown as a ratio of densitometric values. *: p≤0.05.

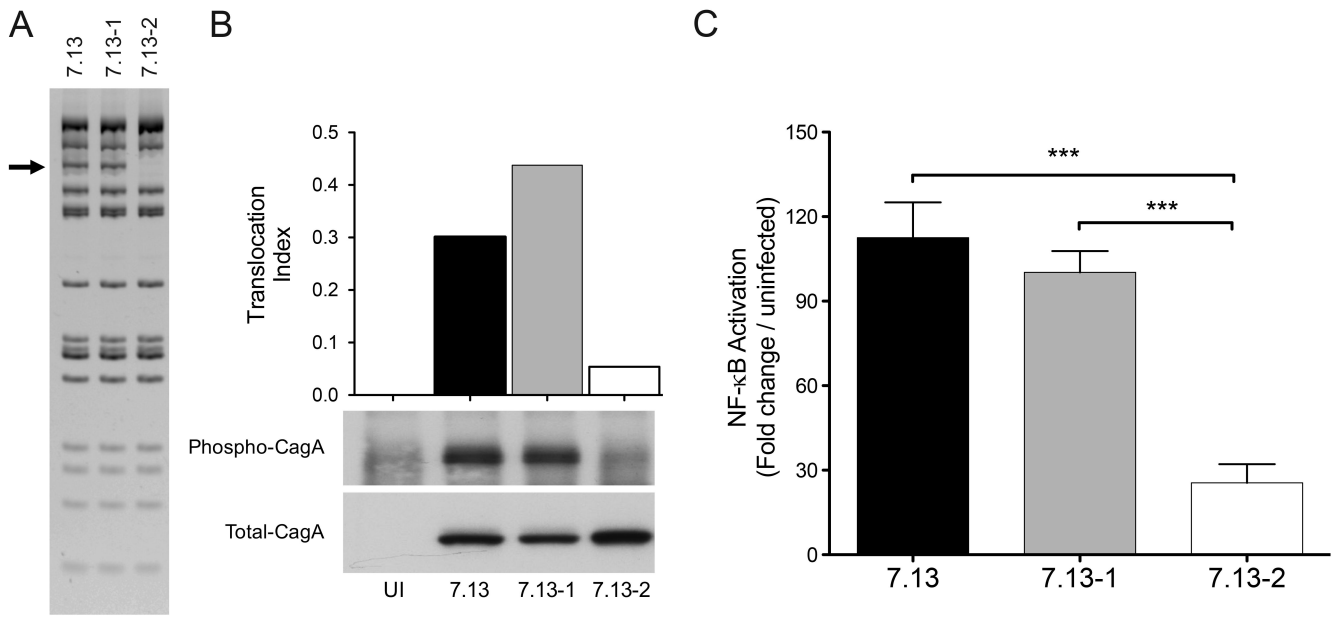

Fig 2. *cag*T4SS function using *H. pylori* output strains from Mongolian gerbils containing different *cagY* rearrangements

(A) *cagY* RFLP profile of *H. pylori* strain 7.13, and its derivative strains 7.13-1 and 7.13-2. (B**)** CagA Western blot of AGS cells co-cultured with *H. pylori* strains 7.13, 7.13-1, and 7.13-2. Translocation index of CagA is the ratio of phosphorylated CagA to total CagA densitometric value. (**C)** NF-κB activation induced by *H. pylori* strains 7.13, 7.13-1, and 7.13-2 after 4 hours of co-culture with AGS cells expressing a Luciferase-based NF-κB reporter. Bars represent mean±SEM of three different assays. Statistical differences were calculated using Mann Whitney test. ***: p≤0.001.

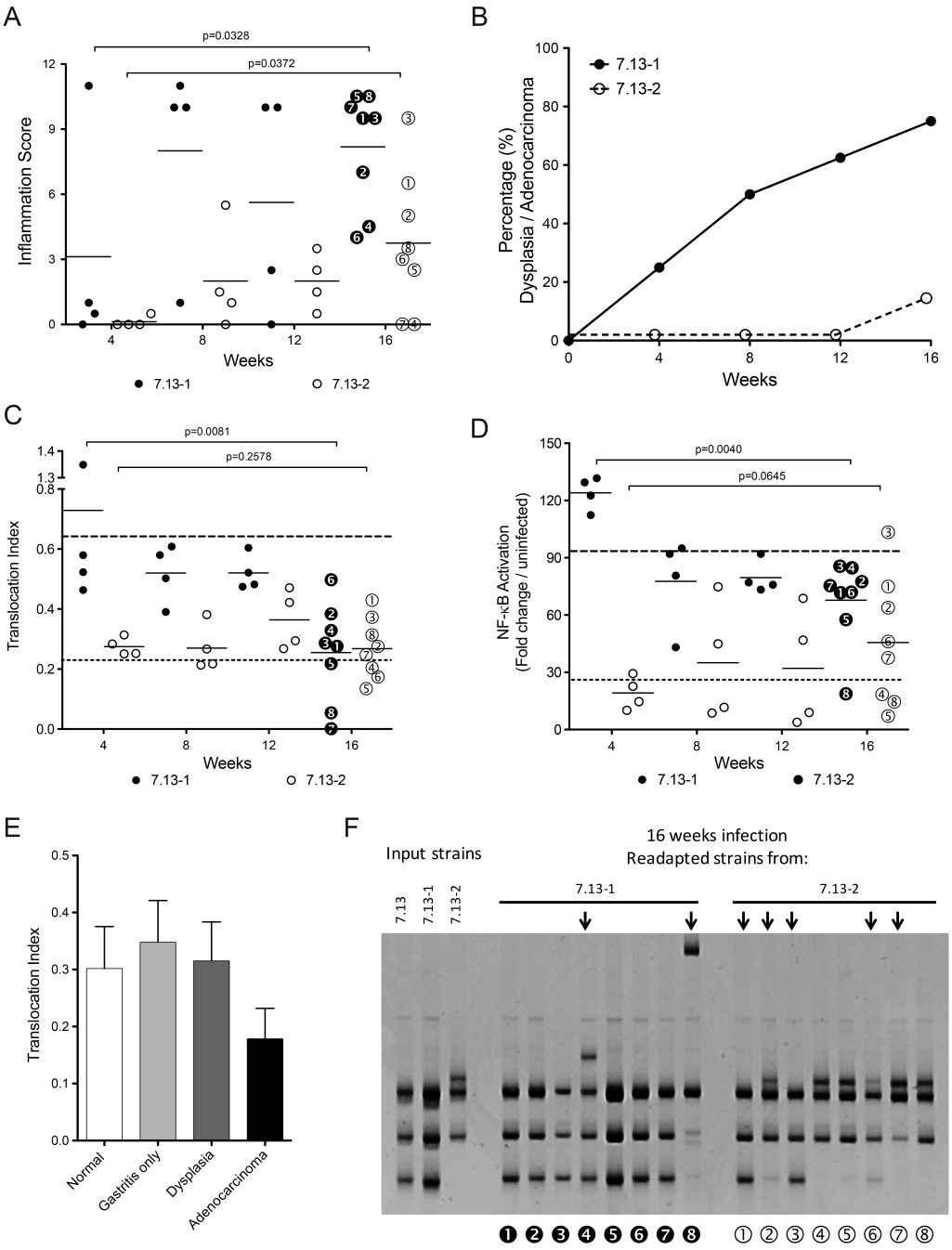

Fig 3. Disease outcome and *cag*T4SS function using *H. pylori* gerbil-adapted strains expressing distinct *cagY* rearrangements

(A) Inflammation scores and **(B)** neoplastic lesions from gerbils infected with *H. pylori* strains 7.13-1 (●) and 7.13-2 (○) for 4, 8, 12, and 16 weeks. **(C)** CagA translocation index and **(D)** NF-κB activation induced by *H. pylori* isolates harvested from gerbils infected with strains 7.13-1 (●) and 7.13-2 (○) for 4, 8, 12, and 16 weeks. Horizontal dotted lines (top line 7.13-1 and bottom line 7.13-2) represent the mean translocation indices of the input strains. **(E)** Gastric injury and CagA translocation indices of *H. pylori* derivative strains

isolated from gerbils infected with strains 7.13-1 or 7.13-2. Bars represent mean±SEM of CagA translocation. (**F)** *cagY* RFLP profiles of *H. pylori* isolates from gerbils after 16 weeks of infection with strains 7.13-1 or 7.13-2. Arrows denote RFLP profiles that differ compared with the corresponding parental strain profile. Numbered black and white circles represent individual *H. pylori* isolates which correspond to isolates shown in panels A, C, and D. Statistical differences were calculated using the Mann–Whitney test.

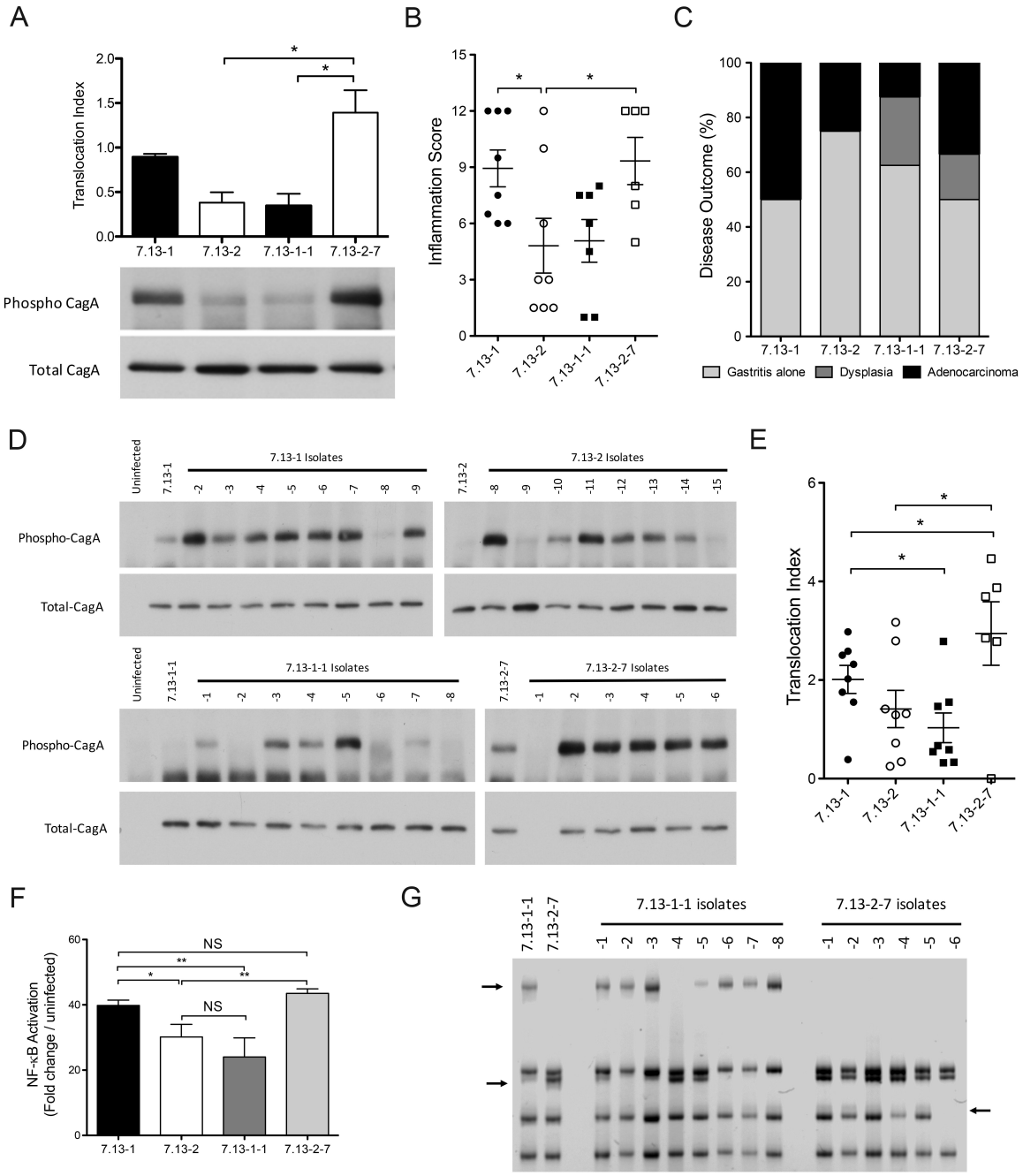

Fig 4. Rearrangements in *cagY* modify *H. pylori cag*PAI function

(A) Translocation index of total and phosphorylated CagA using *H. pylori* strain 7.13-1 and its derivative strain 7.13-1-1, and strain 7.13-2 and its derivative strain 7.13-2-7. Bars represent mean±SEM of CagA translocation from three independent experiments. (**B)** Inflammation scores in gastric tissue from gerbils infected with *H. pylori* strains 7.13-1, 7.13-2, and their derivative strains 7.13-1-1 and 7.13-2-7. (**C)** Disease outcome of gerbils infected with strains 7.13-1, 7.13-2, 7.13-1-1, and 7.13-2-7 for 16 weeks. (**D)** Western blot analysis and **(E)** translocation index for phosphorylated and total CagA in AGS cells co-

cultured with *H. pylori* strains harvested from gerbils infected for 16 weeks with strains 7.13-1, 7.13-2, 7.13-1-1, and 7.13-2-7. (**F)** NF-κB activation induced by *H. pylori* derivative strains isolated from gerbils infected with strains 7.13-1, 7.13-2, 7.13-1-1, and 7.13-2-7 for 16 weeks. (**G)** *cag Y* RFLP profile of *H. pylori* derivatives from gerbils infected with strains 7.13-1-1, and 7.13-2-7 for 16 weeks. Arrows indicate differential bands between isolates. Statistical differences were calculated by One-way Anova using a Newman-Keuls post-test. *: $p \leq 0.05$; **: $p \leq 0.01$. NS: Non-significant.

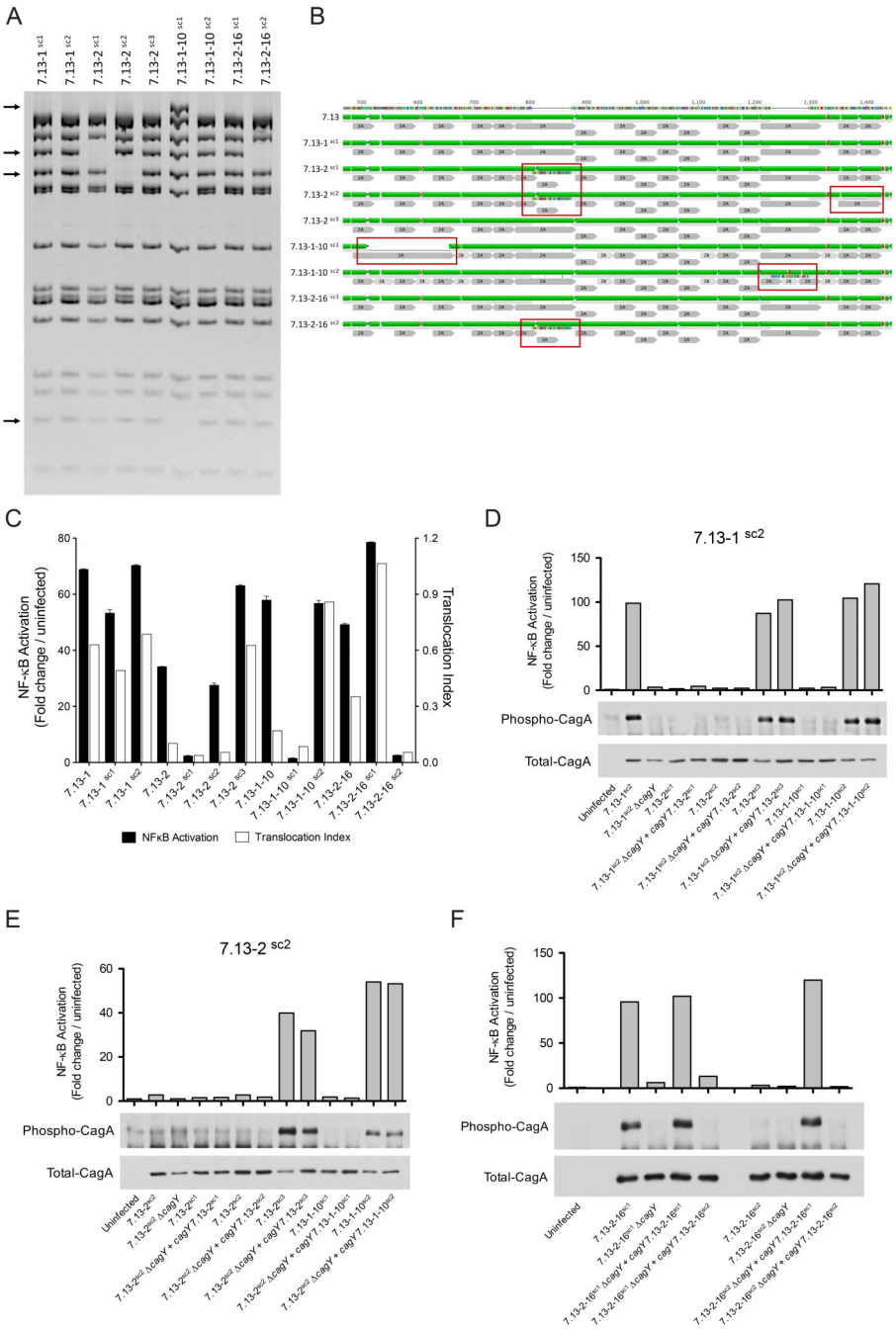

Fig 5. *H. pylori* gerbil-adapted strains represent panmictic populations harboring diverse *cagY* rearrangements

(A) Representative *cagY* RFLP profiles of *H. pylori* single colonies generated from strains 7.13-1, 7.13-2, 7.13-1-10, and 7.13-2-16. Arrows denote differential bands between RFLP profiles. (**B)** Alignment and predicted secondary structure of *H. pylori* CagY parental strain 7.13 and derivative single colony strains. Red boxes highlight gain or loss of motifs 2A and/or 2B compared with parental strain 7.13. Green: alpha helix; purple: beta-sheets, and red: beta turns. Repeat motifs 2A and 2B are in gray. (**C)** NF-κB activation (black bars) and

CagA translocation (white bars) induced by *H. pylori* strains and their corresponding single colony isolates. NF-κB activation, and CagA translocation induced by *H. pylori* strains 7.13-1^{sc2} (**D)** and 7.13-2^{sc2} **(E)** genetically complemented with different *cagY* genes. **(F)** NF-κB activation and CagA translocation induced by *H. pylori* strains 7.13-2-16^{sc1} and 7.13-2-16^{sc2} complemented with either an endogenous *cagY* motif or with a *cagY* motif derived from the sibling strain.

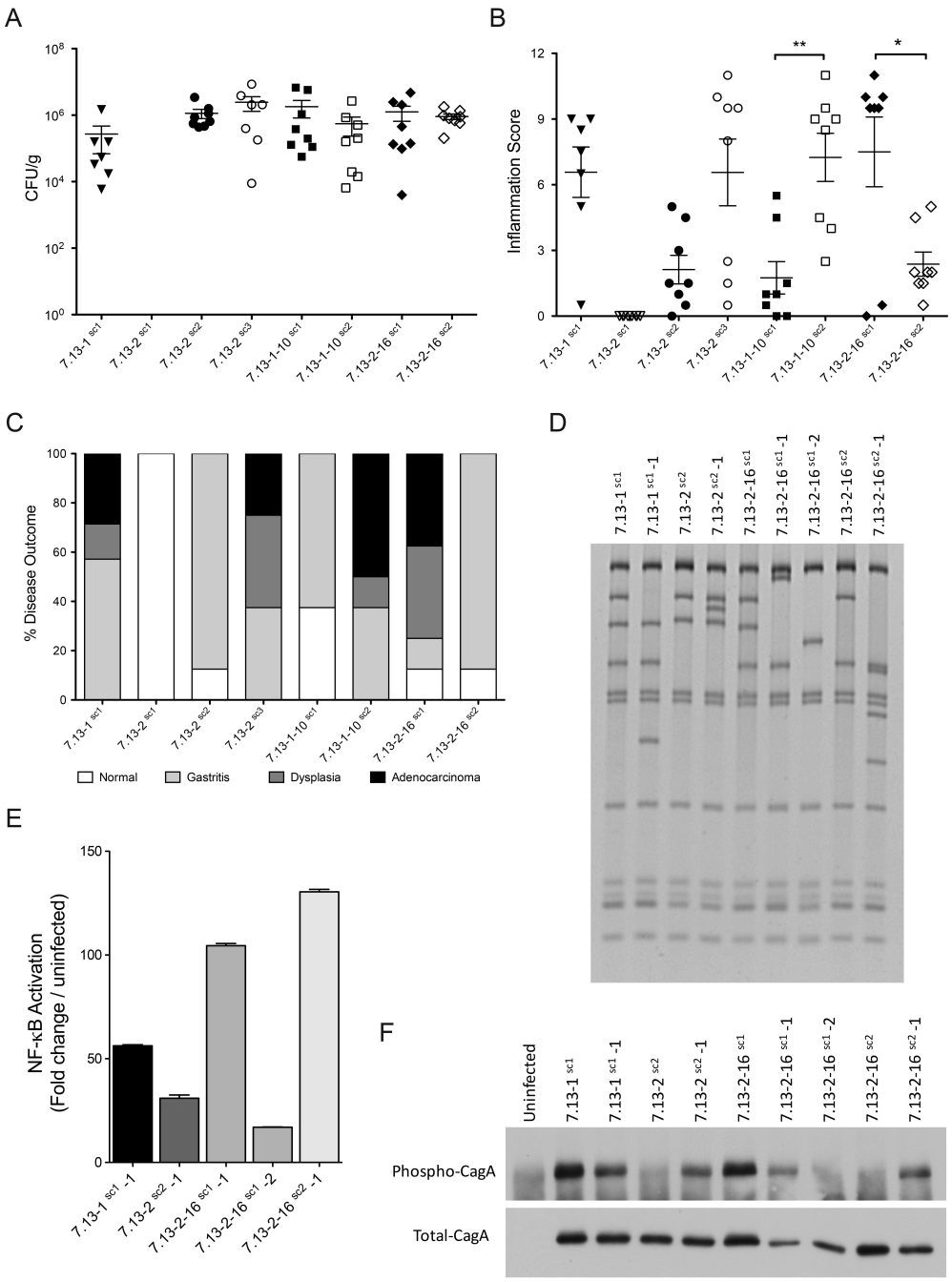

Fig 6. Severity of disease in Mongolian gerbils infected with *H. pylori* single colony isolates and relationship with *cagY* rearrangements

Colonization density **(A),** inflammation scores **(B),** and disease outcome **(C)** of gerbils challenged for 16 weeks with *H. pylori* single colonies carrying specific *cagY* rearrangements. (**D)** *cagY* RFLP profiles, **(E)** NF-**κ**B activation, and **(F)** phosphorylated and total CagA assays of derivative isolates harvested from gerbils infected for 16 weeks with *H. pylori* single colony isolates carrying new *cagY* rearrangements. Statistical differences were calculated by One-way Anova using a Newman-Keuls post-test. *: p≤0.05; **: p≤0.01.

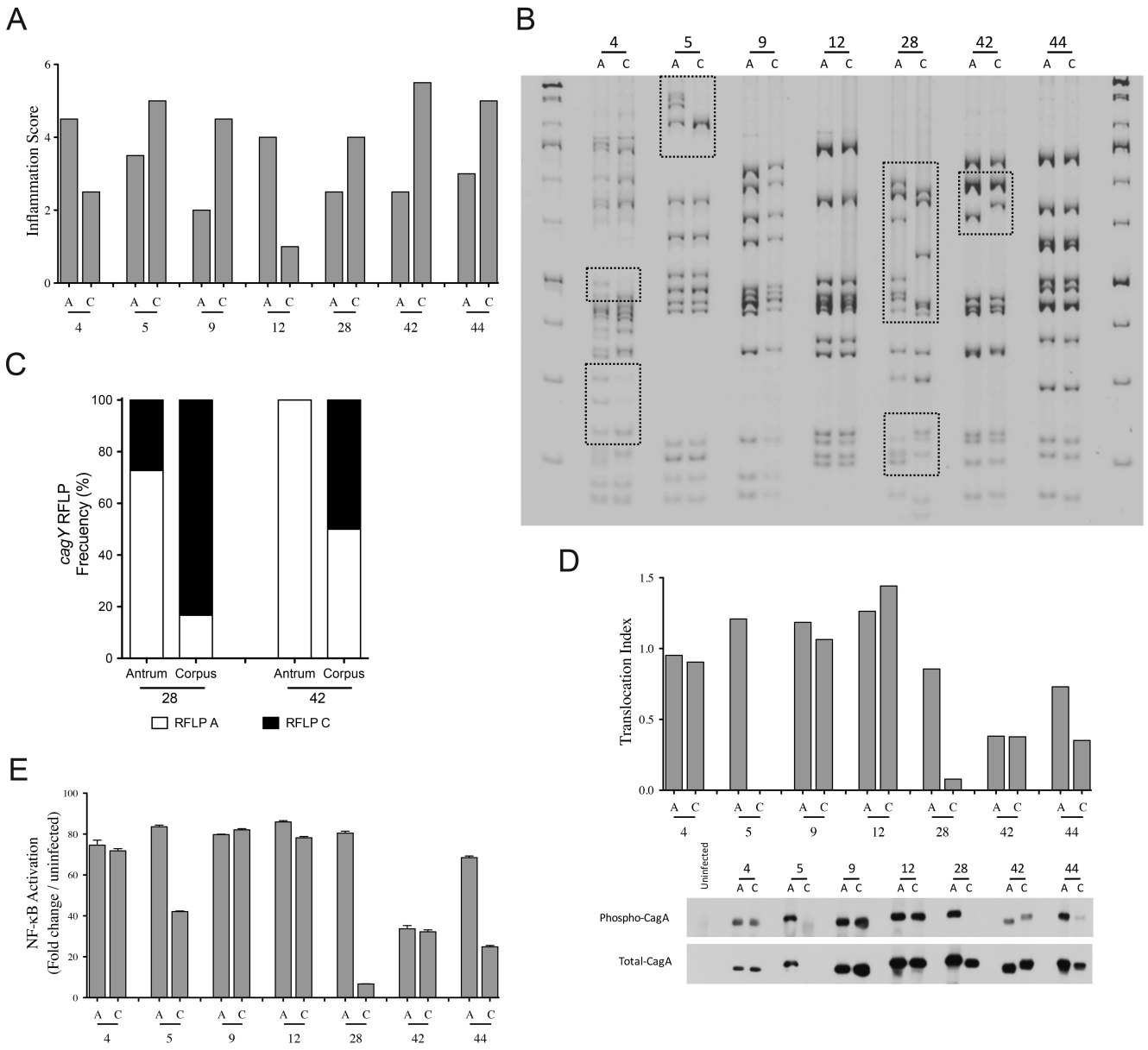

Fig 7. Synchronous *cagY* rearrangements in *H. pylori* clinical isolates

(A) Inflammation scores of human gastric biopsies obtained from the antrum "A" and corpus "C" from the same patient (n=7 patients). **(B)** *cagY* RFLP of *H. pylori* isolates from biopsies obtained from the antrum and corpus of the same patient. Boxes indicate differences in RFLP profiles between sibling strains. **(C)** Frequency distribution of single colony *cagY* genotypes within isolates obtained from the antrum and corpus from two patients (28 and 42). CagA translocation **(D)** and NF-κB activation **(E)** of *H. pylori* isolates from the antrum and corpus of seven patients.